

Amplitude fluctuations due to diffraction and refraction in anisotropic random media: Implications for seismic scattering attenuation estimates

T.M. Müller, S.A. Shapiro, C.M.A. Sick

email: tmueller@geophysik.fu-berlin.de, tobias.muller@geophy.curtin.edu.au

keywords: *anisotropic random media, crustal heterogeneities, scattering attenuation, seismic primaries, diffraction, refraction*

ABSTRACT

We calculate the variance of the log-amplitude within the Rytov approximation for plane waves propagating in weakly inhomogeneous and statistically anisotropic random media. Since there is a simple relation between the log-amplitude variance and the attenuation coefficient of seismic primaries in the weak wavefield fluctuation regime, we also obtain scattering attenuation estimates which additionally depend on the aspect ratio of longitudinal and transverse correlation scales of the inhomogeneities. These estimates can be useful for the statistical characterization of anisotropic, large-scale inhomogeneities (large compared to the wavelength of the probing pulse) in the Earth crust and mantle, such as fault zones. With help of plane-wave-transmission numerical experiments using the finite-difference method we compute the log-amplitude variance as a function of the propagation distance and observe reasonable agreement with the analytical results. We discuss the implications of our results in the context of seismic scattering attenuation estimations.

INTRODUCTION

In seismology it is common practice to analyze the amplitude and phase fluctuations of transmitted and reflected seismic signals in order to statistically characterize the subsurface heterogeneities. In particular, the Rytov approximation for the variance of the log-amplitude and phase fluctuations of diffracted and refracted waves has been applied in several studies (Wu and Flatté, 1990, Sato and Fehler, 1998 and references therein, Tripathi, 2001). For example, Wu and Flatté derived from seismograms of the NOR-SAR array the log-amplitude and phase (and their cross-) correlation function and modeled them with the corresponding correlation functions for isotropic random media. It is well-known that the diffraction and refraction of waves at *randomly* distributed inhomogeneities results in a random focusing and defocusing of wave energy and consequently results in an increase of the amplitude fluctuations with increasing propagation distances (Rytov et al., 1989). Diffraction of seismic waves becomes noticeable if the size of an inhomogeneity exceeds the wavelength. A measure that distinguishes the importance of diffraction and refraction effects is the wave parameter D , which is defined as the ratio of the size of the Fresnel zone and the characteristic length scale of the inhomogeneities (if $D \ll 1$ refraction prevails, whereas for $D \gg 1$ both, diffraction and refraction effects occur). Shapiro and Kneib (1993) showed that the variance of the log-amplitude fluctuations is directly related to the coefficient of scattering attenuation and thus to the scattering quality factor, which is another important quantity in order to characterize the propagation medium.

All the above-mentioned works use the model of an isotropic random medium. There is, however, a lot of evidence that at some sites the heterogeneities of the crust are anisotropic. Indeed, from the analysis

of well-log data at the KTB deep borehole, Wu et al. (1994) suggested a model of randomly distributed velocity inhomogeneities with a lateral characteristic scale of $3.6km$ and a vertical scale of $2km$. Also parts of the lithospheric mantle are assumed to be composed of anisotropic heterogeneities. Ryberg et al. (1995) deduced from short period wavefield data recorded on a profile across Northern Eurasia that this zone contains randomly distributed, spatially anisotropic velocity fluctuations, which are 'stretched' in the horizontal direction. Based on a modeling study of these data, Tittgemeyer et al. (1999) provide a generic description of lower-crust and upper-mantle heterogeneities with a ratio of anisotropy (the aspect ratio of vertical and horizontal correlation scale) of ≈ 0.25 . Analyzing the P-coda characteristics in seismograms from local events at the San Jacinto fault zone, Wagner (1998) concluded that a model of a grossly plane-layered structure statistically described by a spatially anisotropic correlation function would be most consistent with the observations. He raised concern about the 'overlooked alternative' to allow the heterogeneities to be spatially anisotropic. Thus, when analyzing the statistical properties of wavefields recorded in such regions it is necessary to include the anisotropy of the inhomogeneities (this is also pointed out in the book of Sato and Fehler, 1998). Estimates of the strength of the medium perturbations, their correlation properties and of the quality factor will be strongly affected if the model of statically isotropic inhomogeneities is generalized such that also anisotropic inhomogeneities are permitted. To our knowledge, there exist no explicit results how large-scale, anisotropic inhomogeneities affect the amplitudes of seismic primaries.

Kon (1994) presented a qualitative theory of amplitude and phase fluctuations due to diffraction in anisotropic, turbulent media based on the consideration of randomly distributed, collecting and diverging lenses (the isotropic case has been previously discussed in this manner by Rytov et al., 1989). He showed that waves propagating along the short axis of inhomogeneities exhibit decreasing amplitude and phase fluctuations as compared to the isotropic case. Contrarily, waves propagating parallel to the long axis of the inhomogeneities show stronger fluctuations (see Figure 1). In order to describe the statistical moments in weakly inhomogeneous media the Markov and the Rytov approximations are frequently employed (Rytov et al., 1989). Both approximations are restricted by the small-angle scattering (or equivalently forward scattering) assumption. Dashen (1979) argues that the Markov approximation can fail in anisotropic random media because the scattering angles grow successively while the wave passes from one inhomogeneity to the next (this effect is most pronounced when the wave initially propagates along the long axis of the inhomogeneities). It may be suspected that the same argumentation holds for the Rytov approximation. By solving the single scattering problem for anisotropic heterogeneities (with the correlation scales a_x , a_y and a_z , where $a_x = a_z \gg a_y$), Beran and McCoy (1974) showed that for the case $ka_x \gg 1$ (k is the wavenumber) the scattering angles in the directions x, z and y are of the order $\theta_{x,z} = O(\frac{1}{ka_x})$ and $\theta_y = O(\frac{1}{\sqrt{ka_x}})$, respectively. They concluded that a more stringent condition for the validity of small-angle scattering approximations must be imposed as compared with the isotropic scattering problem, where $\theta = O(\frac{1}{ka})$.

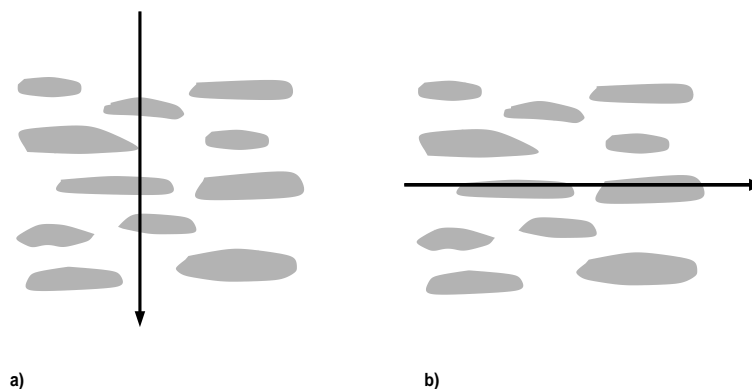


Figure 1: Geometry for wave propagation in anisotropic random media. Two cases are of particular interest: a) main direction of wave propagation parallel to the short axis of the inhomogeneities and b) main direction of wave propagation parallel to the long axis of the inhomogeneities. For both cases we present explicit results of the log-amplitude variance if the inhomogeneities are Gaussian correlated.

In spite of the possibility to treat anisotropic inhomogeneities within the Rytov approximation, usually only final results and discussions for the isotropic case are found (e.g. Ishimaru, 1978, Rytov et al., 1989). Exceptionally, in the works of Komissarov (1964) and Knollman (1964) the anisotropic case is investigated, however resulting in rather complicated expressions for the second order moments of the wavefield. Moreover, Knollman considers the amplitude fluctuations instead of the log-amplitude fluctuations. More recently, the variance of the phase fluctuations, which serves as a measure of the velocity shift, has been analyzed in detail for anisotropic random media by Samuelides (1998). Tractable, explicit results for the log-amplitude variance in the Rytov approximation valid for anisotropic random media are at present not known. It is the purpose of this research note to fill this gap and to discuss its significance in the context of seismic scattering attenuation. That is to say we do not re-derive the Rytov approximation, but on the basis of explicit results (which we numerically verify) we focus on its applicability in anisotropic random media.

The outline of our consideration is the following. First we briefly formulate the problem of seismic scattering in randomly inhomogeneous media in the framework of the stochastic scalar wave equation and provide the basic relations necessary for subsequent sections. Then, an expression of the log-amplitude variance using the Rytov approximation is derived. After that, explicit results for Gaussian random media are presented. The frequency and travel-distance dependency of the log-amplitude variance are analyzed. The analytical results are numerically verified with the help of finite-difference simulations (section last but one). In the last section we discuss our results in the context of seismic scattering attenuation estimates. The results are also discussed in the light of previously obtained approximations for the scattering attenuation coefficient in 3-D isotropic and 1-D random media.

ATTENUATION DUE TO DIFFRACTION AND REFRACTION

In order to study the propagation of waves in randomly inhomogeneous media we use the acoustic wave equation

$$\Delta u(t, \vec{r}) - p^2(\vec{r}) \frac{\partial^2 u(t, \vec{r})}{\partial t^2} = 0 \quad , \quad (1)$$

where we defined the squared slowness as $p^2(\vec{r}) = \frac{1}{c_0^2}(1 + 2n(\vec{r}))$, where c_0 denotes the propagation velocity in a homogeneous reference medium. The function $n(\vec{r})$ is a realization of a stationary random field with zero average, i.e., $\langle n(\vec{r}) \rangle = 0$ and is characterized by a spatial correlation function $B_n(\vec{r}) = \langle n(\vec{r}_1)n(\vec{r}_2) \rangle$ that only depends on the difference vector $\vec{r} = \vec{r}_1 - \vec{r}_2$. A solution of equation (1) in the form of time-harmonic wavefields can be presented using the Rytov transformation

$$u(\omega; \vec{r}) = A_0 e^{\Psi(\omega; \vec{r})} \quad , \quad (2)$$

where the complex function Ψ is composed of the so-called log-amplitude fluctuations

$$\text{Re}\{\Psi\} \equiv \chi \equiv \ln(A/A_0) \quad , \quad (3)$$

and the phase fluctuations $\text{Im}\{\Psi\} \equiv \tilde{\phi} \equiv \phi - \phi_0$. Here the quantities A and ϕ denote the current amplitude and phase, respectively. The quantities A_0 and ϕ_0 define the incident wavefield $u_0 = A_0 \exp(i\phi_0)$ propagating through the homogeneous reference medium ($n(\vec{r}) = 0$).

It has been shown that the mean and the variance of the log-amplitude fluctuations are related through (Rytov et al., 1989)

$$\langle \chi \rangle = -\sigma_\chi^2 \quad , \quad (4)$$

where the variance is defined as $\sigma_\chi^2 \equiv \langle (\chi - \langle \chi \rangle)^2 \rangle$. Equation (4) is valid as long as the wavefield fluctuations are weak and the waves are mainly scattered in the forward direction. Such a regime exists if

$$\sigma_n^2 (ka)^2 \frac{L}{a} < 1 \quad (5)$$

and $ka \geq 1$, where ka and L/a denote the normalized wavenumber and travel-distance, respectively (normalized by the correlation length a). In order to obtain global scattering attenuation estimates, Shapiro

and Kneib (1993) used the fact that the attenuation coefficient α of a plane wave can be expressed through the mean of the log-amplitude fluctuations

$$\alpha = -\frac{\langle \chi \rangle}{L} = \frac{\sigma_\chi^2}{L}. \quad (6)$$

Hence, the key to the description of attenuation due to random diffraction and refraction is the computation of the log-amplitude variance σ_χ^2 . For the case of statistically isotropic random media, in the second-order Rytov approximation one obtains (Ishimaru, 1978)

$$\sigma_\chi^2 = 2\pi^2 k^2 L \int_0^\infty d\kappa \kappa \Phi_n(\kappa) \left[1 - \frac{\sin(\kappa^2 L/k)}{\kappa^2 L/k} \right], \quad (7)$$

where $\Phi_n(\kappa)$ denotes the fluctuation spectrum, i.e. the 3-D Fourier transform of the correlation function B_n .

LOG-AMPLITUDE VARIANCE FOR ANISOTROPIC RANDOM MEDIA

The calculation of the variance of the log-amplitude fluctuations is based on that for the transverse correlation function $B_\chi = \langle \chi \chi^* \rangle$, because by definition $\sigma_\chi^2 \equiv B_\chi(\vec{\rho} = 0)$, where $\vec{\rho}$ denote the spatial coordinates transversal to the direction of the incident wave (x -direction). The log-amplitude correlation function at zero lag is given by the following expression (Ishimaru, 1978, equation 17.44)

$$\sigma_\chi^2 = k^2 \int_0^L dx' \int_0^L dx'' \iint d\vec{\kappa} F_n(x' - x'', \vec{\kappa}) \sin\left(\frac{L-x'}{2k} \kappa^2\right) \sin\left(\frac{L-x''}{2k} \kappa^2\right), \quad (8)$$

where F_n denotes the 2-D Fourier transform of the correlation function B_n in the transverse coordinates $\vec{\rho}$

$$F_n(x' - x'', \vec{\kappa}) = \frac{1}{4\pi^2} \iint B_n(x' - x'', \vec{\rho}) e^{-i\vec{\kappa}\vec{\rho}} d\vec{\rho}. \quad (9)$$

Note that equation (8) and (9) are also valid in the general case when the direction of wave propagation x does not coincide with the axes of the correlation lengths of the inhomogeneities. In this case the correlation function B_n can be transformed such that the angle between planes transversal to the direction of propagation and the planes spanned by the axes of the correlation lengths is included (see e.g. Samuelides, 1998).

In a next step, the difference and center-of-mass coordinates $x_d = x' - x''$ and $\eta = \frac{x' + x''}{2}$ are introduced and the ranges of integration are transformed according to equation (17.46) of Ishimaru (1978): $\int_0^L dx' \int_0^L dx''(\cdot) \approx \int_0^L \eta \int_{-\infty}^\infty dx_d(\cdot)$. In the derivation of σ_χ^2 for the isotropic case it is assumed that the 'sin' terms in equation (8) are slowly varying functions of x' and x'' because $\kappa^2 a/k < 1/ka \leq 1$ and therefore these variables are replaced by the center-of-mass coordinate η , i.e. $\sin\left(\frac{L-x'}{2k} \kappa^2\right) \sin\left(\frac{L-x''}{2k} \kappa^2\right) \approx \sin^2\left(\frac{L-\eta}{2k} \kappa^2\right)$. However, this replacement means that local variations of the medium parameters in the direction of wave propagation are not taken into account and consequently the correlation length in the direction of wave propagation, a_{\parallel} becomes a redundant parameter. This is admissible in isotropic random media, where it is known that the correlation length transversal to the direction of wave propagation, a_{\perp} , mainly controls the strength of the wavefield fluctuation (Ishimaru, 1978, chapter 20). Considering anisotropic random media, more accurate results can be obtained when all terms inside the 'sin' functions in equation (8) are retained when introducing the center-of-mass coordinate η . Thus, we have $\sin\left(\frac{L-x'}{2k} \kappa^2\right) \sin\left(\frac{L-x''}{2k} \kappa^2\right) = \cos^2\left(\frac{x_d}{4k} \kappa^2\right) - \cos^2\left(\frac{L-\eta}{2k} \kappa^2\right)$. Performing now the integration with respect to η , equation (8) modifies to

$$\sigma_\chi^2 = k^2 L \iint d\vec{\kappa} \int_0^\infty dx_d F_n(x_d, \vec{\kappa}) \left[\cos^2\left(\frac{x_d}{2k} \kappa^2\right) - \frac{\sin(\kappa^2 L/k)}{\kappa^2 L/k} \right]. \quad (10)$$

This equation has a similar structure as compared with the isotropic result (7), however, involves an additional integration with respect to the difference coordinate x_d , which can not be performed without specifying the correlation function B_n and hence F_n . Equation (10) together with equation (6) provides an estimate of the scattering attenuation coefficient of seismic primaries in anisotropic random media. A similar equation can be obtained for 2-D random media. In particular, dividing equation (10) by π , and using the 1-D Fourier transform of B_n instead of equation (9) yields the 2-D result for σ_χ^2 . We note that the variance of the phase fluctuations, the crossvariance between log-amplitude and phase fluctuations and also the transverse correlation functions can be treated in the same manner. This is, however, not the topic of the present study.

EXPLICIT RESULTS FOR GAUSSIAN RANDOM MEDIA

In order to obtain explicit results from equation (10) we have to specify the correlation function B_n . We choose a Gaussian correlation function $B_n(\vec{r}) = \sigma_n^2 \exp\left(-\frac{x^2}{a_x^2} - \frac{y^2}{a_y^2} - \frac{z^2}{a_z^2}\right)$. For simplicity, we consider the case of wave propagation in x direction so that the correlation length parallel to this direction is $a_{||} = a_x$ and assume also that $a_y = a_z = a_\perp$, i.e. isotropy in the transversal plane. Then, the correlation function is of the form

$$B_n(\vec{r}) = \sigma_n^2 \exp\left(-\frac{x^2}{a_{||}^2} - \frac{\rho^2}{a_\perp^2}\right) \quad (11)$$

and with help of equation (9), which in the given geometry degenerates to the Hankel transform, one obtains

$$F_n(x_d, \kappa) = \sigma_n^2 \frac{a_\perp^2}{4\pi} \exp(-x_d^2/a_{||}^2) \exp(-\kappa^2 a_\perp^2/4). \quad (12)$$

Inserting equation (12) into (10) and performing the integrations with respect to x_d and κ , we obtain

$$\sigma_\chi^2 = \sigma_n^2 \frac{\sqrt{\pi}}{16} k^4 a_\perp^4 \left(\sqrt{\pi} e^{1/A^2} [1 - \text{erf}(1/A^2)] 2D - A \arctan(2D) \right), \quad (13)$$

where erf denote the error function and we introduced the dimensionless quantities $D = \frac{2L}{ka_\perp^2}$ (known as the wave parameter) and $A = \frac{2a_{||}}{ka_\perp^2}$. For $ka_\perp > 1$, which is required in order to satisfy restriction (5), equation (13) can be simplified

$$\sigma_\chi^2 \approx \sigma_n^2 \frac{\sqrt{\pi}}{4} \frac{a_{||}}{a_\perp} k^3 a_\perp^3 D \left[1 - \frac{\arctan(2D)}{2D} \right]. \quad (14)$$

An analogous calculation yields the 2-D result

$$\sigma_\chi^2 \approx \sigma_n^2 \frac{\sqrt{\pi}}{4} \frac{a_{||}}{a_\perp} k^3 a_\perp^3 D \left[1 - \frac{1}{\sqrt{2}D} \sqrt{\sqrt{1+4D^2} - 1} \right]. \quad (15)$$

It is interesting to note that in the case $a_{||} = a_\perp$, formulas (14) and (15) exactly coincide with the formulas of σ_χ^2 for the isotropic case (e.g. Müller et al., 2002). Therefore, the ratio $\gamma = \frac{a_{||}}{a_\perp}$ additionally controls the magnitude of the log-amplitude variance in anisotropic random media. Equations (14) and (15) for the variance of the log-amplitude complement the corresponding equations for the variance of the phase fluctuations (see equations (20) and (29) in Samuelides, 1998). Figure (2) shows the log amplitude variance according to equation (14) as a function of the wave parameter for a fixed value of ka_\perp but varying parameter γ .

With increasing travel-distances the wavefield fluctuations also increase. Once reached the strong wavefield fluctuations regime (the quantity $\sigma_n^2 (ka)^2 \frac{L}{a}$ is comparable or larger than unit), it is well-known that the variance of the intensity fluctuations m^2 (the so-called scintillation index) saturates, i.e., $m^2 \rightarrow 1$ if $\sigma_n^2 (ka)^2 \frac{L}{a} = O(1)$ (Rytov et al., 1989). It is easy to show that the variance of the intensity fluctuations and that of the log-amplitude fluctuations are related via $m^2 = \exp(4\sigma_\chi^2) - 1$ (Shapiro and Kneib, 1993).

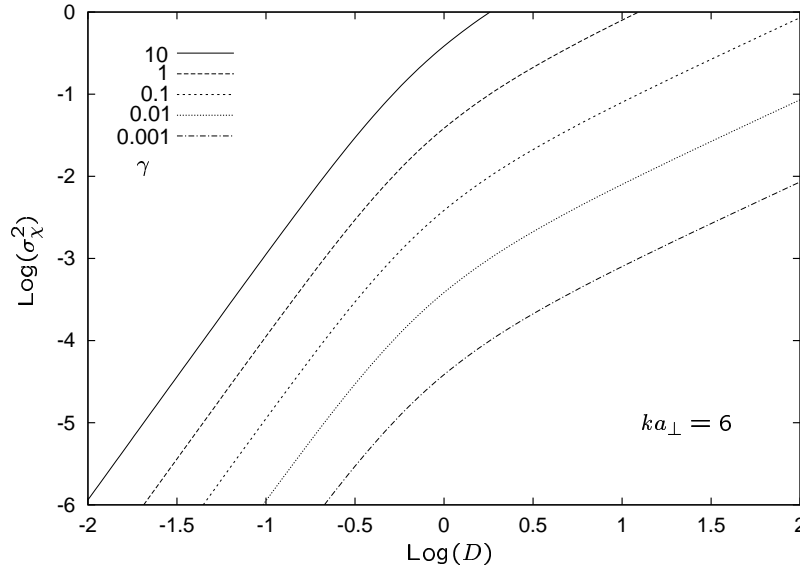


Figure 2: The normalized log-amplitude variance (14) as a function of the wave parameter for varying γ and fixed ka_{\perp} . Compared to the isotropic case ($\gamma = 1$), σ_{χ}^2 is increased for $\gamma > 1$ and decreased for $\gamma < 1$. The characteristic dependence on the wave parameter D is the same for all γ . For $D \ll 1$, $\sigma_{\chi}^2 \propto D^3$, whereas for $D \gg 1$, $\sigma_{\chi}^2 \propto D$ (see the discussion in Rytov et al., 1989).

Consequently, for $m^2 \rightarrow 1$ the log-amplitude variance tends to the constant $\frac{1}{4} \ln(2) = 0.173$. This result is true if the incident wave has unit intensity and backscattering can be neglected. A different constant is obtained for anisotropic random media: Taking into account the results for isotropic and anisotropic random media (denoted by $^{\text{iso}}\sigma_{\chi}^2$ and $^{\text{aniso}}\sigma_{\chi}^2$, respectively), we roughly obtain $^{\text{aniso}}\sigma_{\chi}^2 \approx \gamma \cdot ^{\text{iso}}\sigma_{\chi}^2$ and thus the log-amplitude variance tends to the constant

$$\sigma_{\chi}^2 \cong \frac{1}{4\gamma} \ln(2). \quad (16)$$

This constant depends on the correlation properties in longitudinal and transversal directions. If $\gamma \gg 1$, this constant is much smaller than that of the isotropic case indicating that a saturation of the log-amplitude fluctuations occurs at shorter propagation distances. However, in such a case the neglect of backscattered energy is not any more admissible (because the scattering angles will not be any more small) and the total amount of wavefield energy received at geophones transverse to the direction of wave propagation decreases with increasing propagation distances. If $\gamma < 1$ the constant value (16) is larger than that in isotropic random media. This behavior is numerically verified in the section below. Note that in the case $\gamma \ll 1$ equation (16) is again not any more valid because the Rytov approximation for σ_{χ}^2 in 3-D does not take into account backscattered waves (see also the discussion in the next paragraph).

From equations (14) and (15) we can roughly estimate the range of applicability of equation (10). For the isotropic case, i.e. $\gamma = 1$, inequality (5) must be satisfied. For the anisotropic case ($\gamma \neq 1$), it is natural to assume that inequality (5) extends to

$$\sigma_n^2 \frac{a_{\parallel}}{a_{\perp}} (ka_{\perp})^2 \frac{L}{a_{\perp}} < 1. \quad (17)$$

As a consequence, if $\gamma < 1$, the log-amplitude variance (10) can be applied for larger travel-distances as compared with the isotropic case. The opposite is true if $\gamma > 1$. Then, one should observe stronger wavefield fluctuations as compared to the isotropic case. This is in agreement with the calculations of Kon (1994) and Beran and McCoy (1974). Note that relation (17) in fact does not depend on the transverse correlation length a_{\perp} and thus the validity range is formally the same as in (5) provided that the correlation

length a is replaced by the correlation length in the direction of wave propagation $a_{||}$. Although the wave apparently interacts with the transverse correlation scale, the strength of the log-amplitude fluctuations is controlled by the longitudinal correlation scale $a_{||}$. There is an additional restriction for the applicability of equation (10), which results from the fact that backscattered waves are neglected within the Rytov approximation in 2-D and 3-D random media. It can be formulated as

$$\begin{cases} ka_{\perp}\gamma > 1 & \text{if } \gamma < 1 \\ ka_{\perp} > 1 & \text{if } \gamma > 1 \end{cases} \quad (18)$$

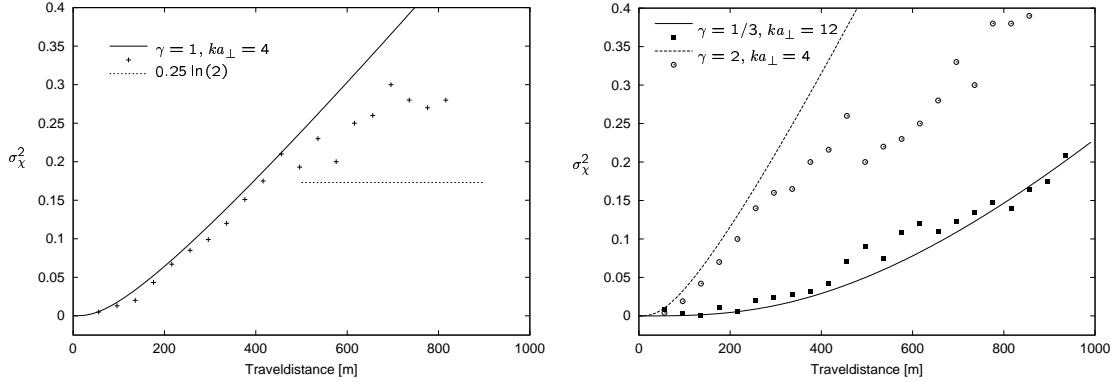
and is analogous to the condition $ka > 1$ in the isotropic case. The meaning of this constraint is also discussed in the last section. In conclusion, equations (17) and (18) define the validity range of formula (10).

NUMERICAL VERIFICATION

In order to verify equations (14) and (15), we perform finite-difference simulations of wave propagation in 2-D random media. Similar numerical experiments have been performed by Shapiro and Kneib (1993) and Müller et al. (2002) for isotropic random media. Results of numerical simulations of seismic waves in anisotropic random media are also presented in Ikelle et al. (1993). In this study, a plane wave (a Ricker wavelet with a dominant frequency of $43Hz$) propagating in the homogeneous reference medium ($c_0 = 3000m/s$ and $n(\vec{r}) = 0$) impinges on a slab of an anisotropic random medium realization, where the inhomogeneities are Gaussian correlated (with a standard deviation of 5% and correlation scales specified below). The long (short) axis of the inhomogeneities is perpendicular to the direction of wave propagation. Inside the random medium the initially plane wave field becomes distorted and is recorded by 20 receiver lines perpendicular to the main propagation direction. Each receiver line consists of 150 geophones separated by the distance of the horizontal correlation length. The log-amplitude variance is extracted from the synthetic seismograms in the following way. 1) A box-car window is applied around the primary arrivals. The window length increases with increasing travel-distance (this is in accordance with the results of Müller and Shapiro, 2001), where it is shown that the broadening of the primaries is approximately proportional to \sqrt{L} . 2) The amplitude spectrum of the windowed seismograms is calculated. 3) We take the logarithm of the amplitude spectra and subtract the logarithm of the amplitude spectrum of the incident pulse. 4) We average the resulting quantity over all geophones along one receiver line. Repeating this procedure for all receiver lines yields the desired log-amplitude variance as a function of travel-distance (using equation (4)).

The numerical results are displayed in Figure (3). To emphasize the differences with the isotropic case, we performed a reference experiment (i.e. $a_{||} = a_{\perp} = 45m$) for which the evaluated log-amplitude variance is shown in the plot on the left hand side (Figure 3(a)). Up to travel-distances of $500m$ the numerical results (illustrated by crosses) closely follow the theoretical prediction (the solid line), i.e. equation (15) with $\gamma = 1$. For travel-distances larger than $500m$ the weak fluctuation regime is not any more valid (restriction (17) yields for $L = 500m$ a value of $\sigma_{\chi}^2 \approx 0.5$), and the σ_{χ}^2 estimate for the strong fluctuation regime roughly applies (the constant $0.25 \ln(2)$ is indicated by the dotted line). That the numerically determined values slightly exceed this constant value is caused by numerical instabilities during the computation of σ_{χ}^2 and by the choice of the window length. Nevertheless, there is an indication of the saturating behavior of σ_{χ}^2 at the level ≈ 0.2 .

The numerical results for anisotropic media are displayed in Figure (3(b)). In a further experiment we choose $a_{||} = 90m$ and $a_{\perp} = 45m$ so that $\gamma = 2$ and as predicted by equation (15) the σ_{χ}^2 values grow more rapidly with travel-distance (the dotted line and diamonds, respectively). It can be also observed that the range of weak fluctuation regime is restricted by smaller travel-distances as compared to the isotropic case (in agreement with restriction (17)). The strong fluctuation regime apparently begins at $L \approx 300m$, however there is no indication of a saturation of the log-amplitude variance. This is probably caused by two reasons. First, as in the isotropic case the numerical evaluation of σ_{χ}^2 becomes less accurate when the wavefield fluctuations are too strong. Second, as mentioned in the introduction, for wave propagation along the longer axis of the inhomogeneities it is known that the scattering angles are not any more small



(a) Results for a reference experiment in isotropic random media (the solid line denotes σ_χ^2 according to equation (15), the crosses denote the numerically determined values).

(b) Here, the results for σ_χ^2 in anisotropic random media for two values of $\gamma = a_{||}/a_\perp$ are presented (the lines correspond to formula (15), the diamonds and rectangles denote the corresponding numerical results).

Figure 3: The log-amplitude variance as a function of travel-distance. Apart from the correlation lengths, the medium parameters are in all experiments the same: $c_0 = 3000m/s$, $\sigma_v = 0.05$ and the value of k is derived from the dominant frequency of $43Hz$.

and thus there is a considerable amount of backscattering which is neglected in the consideration of the strong-fluctuation-regime estimate of σ_χ^2 (see also last paragraph of the section above). Further numerical considerations (results are not shown) indicate that for even larger values of γ the presented formulas cannot be any more applied (in agreement with restriction (17)). A common travel-distance gather for $L = 500m$ is displayed in Figure (5) (bottom) showing a strongly distorted primary wave, which is a qualitative indication for these strong wavefield fluctuations.

The numerical results for wave propagation along the short axis of the inhomogeneities is also displayed in the plot on the right hand side of Figure (3). Here, we choose $a_{||} = 45m$ and $a_\perp = 135m$ so that $\gamma = 1/3$. The numerically determined σ_χ^2 values (the filled squares) fit the theoretical result given by equation (15) (the solid line) quite well over the whole travel-distance interval under consideration ($L = 0..1000m$). This is again in agreement with restriction (17), which predicts a increased range of validity of the Rytov approximation for wave propagation along the shorter axis of the inhomogeneities ($\gamma < 1$). In this case, the regime of strong wavefield fluctuations is beyond the domain of our numerical simulation. That the numerical estimates of σ_χ^2 fluctuate slightly stronger around the theoretical curve as compared to the isotropic case is a purely numerical effect because less statistically independent measurements are made (i.e. the distance between two geophones is less than the horizontal correlation length).

In order to elucidate the increased range of applicability of the Rytov approximation for σ_χ^2 (and to assess its limitations) we perform further experiments. First, we repeat the last experiment with $\gamma = 1/3$, however, for a medium with stronger velocity fluctuations ($\sigma_v = 10\%$). The extracted log-amplitude variances are shown in Figure (4(a)) by the black squares. The theoretical prediction is shown by the solid curve, which gives a good approximation for the numerically determined values up to $L \approx 500m$. For larger travel-distances we observe a saturating behavior of the log-amplitude variances, indicating the beginning of the strong fluctuation regime. Comparing this result with that of the corresponding isotropic case, where $\sigma_v = 5\%$ (displayed at Figure (3(a))), we observe the same range of travel-distances, where formula (15) gives a good approximation in spite of the fact that σ_v is twice as large. This is in agreement with equation (17): in anisotropic random media with $\gamma < 1$ we may increase the medium contrasts without violating the range of applicability. There is however a significant difference for the two experiments regarding the magnitude of the log-amplitude variances. Also the level of saturation has been increased for the experiment with $\gamma = 1/3$ (now $\sigma_\chi^2 \approx 0.35$ instead of 0.2 for the experiment with $\gamma = 1$). This increase

can be qualitatively explained using estimate (16) (the experiment shows that it is only a rough estimate because we expect $\sigma_\chi^2 \text{sat} = \frac{3}{4} \ln(2) \approx 0.5$).

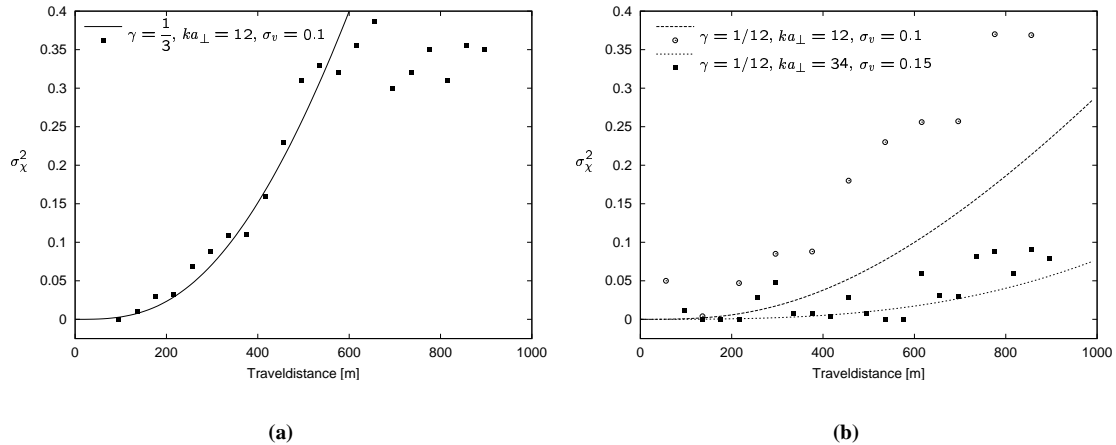


Figure 4: The log-amplitude variance as a function of travel-distance determined from experiments, where the limits of applicability are reached (see main text for explanation). In a) and b) we used $c_0 = 3000\text{m/s}$ and a dominant frequency of 43Hz . The strength of the perturbations and the ratio of spatial anisotropy are indicated in the legend.

Decreasing γ , increases the range of applicability of the formulas for σ_χ^2 . However, arbitrary small values of γ are only admitted if, at the same time, the conditions (17) and (18) are satisfied. This is demonstrated by the following examples. Choosing $\sigma_v = 10\%$, $a_\perp = 135\text{m}$ and $a_\parallel = 11.25\text{m}$ (we then have $\gamma = 1/12$), the resulting values of σ_χ^2 are displayed by the unfilled circles in Figure 4(b). The theoretical prediction is plotted as dashed line. Obviously, there is no more agreement between theory and experiment. The reason for this discrepancy is the violation of condition (18) (now $ka_\parallel \leq 1$). In such a model we expect a significant contribution to the attenuation due to scattering at quasi 1-D inhomogeneities and a reduced contribution due to random diffractions and refractions (see discussion in the next section). The change in the significance of the physical mechanism which causes attenuation becomes also visible in the spatial energy-redistribution of waves propagating in an inhomogeneous medium. The uppermost plot in Figure(5) displays a common-travel-distance gather for the experiment under consideration. Apart from random diffractions (visible through fluctuating amplitudes for a fixed time), the wave field behind the primary wave is composed of 'multiples' that are similar in shape (but reduced in amplitude) as compared with the primary wave. A quite different picture gives the common-travel-distance gather for a reference experiment, where condition (18) is satisfied (middle plot in Figure 5). Here the wavefield fluctuations are concentrated in the vicinity of the wavefront which is, however, more distorted than that of the previous experiment. Moreover, the randomly distributed diffractions and refractions are clearly visible. In such a situation the presented formulas for σ_χ^2 can be applied. This is also demonstrated in an experiment with $\sigma_v = 15\%$, where condition (18) is met ($a_\perp = 360\text{m}$ and $a_\parallel = 30\text{m}$), however, due to the strong fluctuations we reach the limit of condition (17) (now $\sigma_v^2(ka_\parallel)^2 L/a_\parallel \geq 1$ for $L \geq 200\text{m}$). As a consequence, the numerically determined values of σ_χ^2 slightly exceed the theoretical prediction (see the squares and the dotted line in Figure 4(b) and the corresponding seismogram section in Figure (5)).

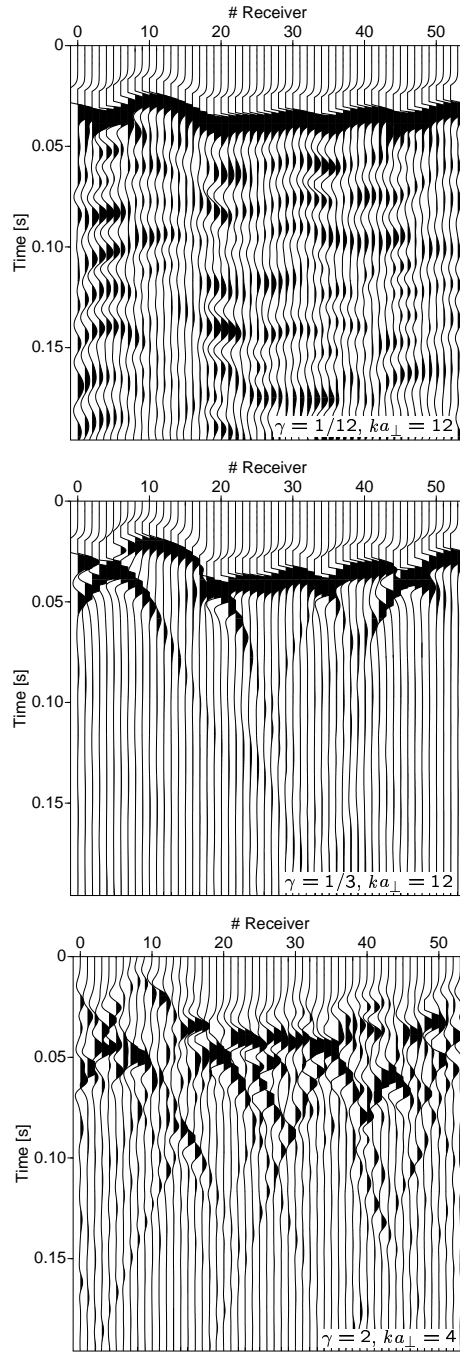


Figure 5: Simulated common-travel-distance gather ($L = 500m$) in anisotropic random media ($c_0 = 3000m/s$) with varying γ (indicated at the lower right corner of each plot) and fixed perturbation strength ($\sigma_v = 0.1$). Top: Condition (18) is violated and the random diffractions and refractions are superimposed with spatially coherent 'multiple reflections'. Middle: Conditions (17) and (18) are satisfied and the formulas for the σ_χ^2 work well. Bottom: Condition (17) is violated and the beginning of the strong fluctuation regime becomes visible through the decomposition of the clearly distinguishable ballistic wave (the primary wave) into random fluctuations.

DISCUSSION

That the log-amplitude variance calculated in the Rytov approximation serves as an estimate of attenuation due to diffraction and refraction at randomly distributed velocity inhomogeneities (in connection with equation (6)) becomes once more evident when we consider the limit $a_{\perp} \rightarrow \infty$ (while a_{\parallel} remains finite), which corresponds to a purely layered random medium. In such a case, the log-amplitude variance vanishes and resembles the fact that in 1-D random media no diffraction effects nor random foci due to refraction (nor intersecting 'rays') occur. Thus, in addition to the limits of applicability of the Rytov approximation to estimate the amount of scattering attenuation (weak wavefield fluctuations), there is a further constraint in anisotropic random media: For a certain ratio of anisotropy ($\gamma \ll 1$) and for wavelengths that exceed the correlation distance in the direction of wave propagation those diffraction and refraction effects, which cause amplitude fluctuations along the direction perpendicular to the direction of propagation, play a minor role. Then, the attenuation of primary waves is mainly caused due to backscattering and primary amplitudes are given by constructive interference of parts of the wavefield that are multiply reflected and refracted (transmitted) at quasi 1-D impedance contrasts. This resembles the physics of scattering attenuation in 1-D random media, which is maximal for $ka = 1$ and is larger than in 2-D and 3-D random media if $ka < 1$ (because of the universal Rayleigh scattering frequency dependence $\alpha \propto \omega^{d+1}$, where d denotes the spatial dimension). That is why the description of scattering attenuation of primary waves within the Rytov theory in 2-D and 3-D anisotropic random media is principally limited by the neglect of backscattering (constraint 18).

It is interesting to relate the above description of scattering attenuation of primaries in anisotropic random media to existing full-frequency-range-valid approximations, which have been obtained for 3-D isotropic random media on the one hand and 1-D random media on the other. For 3-D (and also 2-D) isotropic random media Müller et al. (2002) derived within the weak scattering regime a solution for the scattering coefficient α , which is attached to the most probable primary pulse (note that in 3-D there is a multitude of possible realizations of primary pulses). This dynamic solution of α has been obtained by combining the Rytov approximation (compare with equation (7) for the log-amplitude variance) with another perturbation approximation that partially takes into account backscattering. In contrast to this, the present results are only based on the Rytov approximation, which completely neglects backscattered waves and thus restricts the validity of α with respect to the frequency range as discussed in the previous paragraph. For 1-D random media Shapiro and Hubral (1999) obtained approximations of the scattering attenuation coefficient within the so-called *generalized O'Doherty-Anstey* (ODA) approach. This is formally equivalent to the second-order Rytov approximation for 1-D random media, which has the remarkable property to account for backscattered waves. A general description of scattering attenuation in 3-D anisotropic random media, which reduces in the layered-media-limit to the results of the ODA approach, has not been reported so far. However, we think that the present results are a first step towards this goal.

The quantification of seismic scattering attenuation along with estimates of the correlation scales and the spatial orientation of subsurface heterogeneities in the crust and mantle may contribute to the understanding of large-scale geoprocesses. Wrong estimates of scattering attenuation can lead to serious misinterpretations of rock properties and structural images. If there is evidence for the presence of anisotropic inhomogeneities (which in many geological settings is the case, see introduction), these information must be taken into account in the calculation and interpretation of scattering attenuation. The above results can also provide a useful correction to the scattering attenuation estimates obtained from seismo-stratigraphic considerations when additionally the finite lateral extent of geological structures is taken into account. The combination of the scattering attenuation descriptions for 1-D and 3-D random media is the topic of a forthcoming paper.

In Müller and Shapiro (2001) scattering attenuation estimates for the German KTB area were obtained with help of statistical estimates of velocity inhomogeneities deduced from the well-log data. With the assumption of statistically isotropic inhomogeneities, they explained a large amount of the 'measured' attenuation (extracted from the seismic data of the accompanying VSP experiment) in terms of scattering. A previously reported hypothesis Lüschen et al. (1993) assumes that seismic reflectivity is mainly related to scattering at hydraulically active fracture zones. We hypothesize that such fracture systems can effectively act like an anisotropic random medium, where the largest correlation scale is associated with the average

direction of the fractures and cracks. Moreover, to assume spatially anisotropy is necessary because in fracture systems there is a preferred orientation of cracks that is associated with the orientation of major faults. Taking into account the steeply inclined major faults in the KTB region (for depths up to 10 km the dip angle is typically $30-70^\circ$, see e.g. Harjes et al., 1997), it is reasonable to assume that the seismic waves in the VSP experiment traveled to some extent parallel to the cracks and thus along the long axis of the anisotropic random medium such that the case $\gamma > 1$ applies. For the evaluation of scattering attenuation this has an important consequence. As shown above, for $\gamma > 1$ larger scattering attenuation estimates are obtained as compared to the isotropic case. Taking into account this fact, we speculate that the amount of scattering attenuation at the KTB area can be even larger than that evaluated in Müller and Shapiro (2001)).

CONCLUSIONS

In conclusion, we derived tractable results for the log-amplitude variance in anisotropic random media based on the Rytov approximation. Assuming Gaussian correlated inhomogeneities we obtain explicit results, which are confirmed by numerical simulations. For wave propagation along the large axis of inhomogeneities, the Rytov approximation is not the best choice because of its limited range of validity. The opposite is true for wave propagation along the short axis of the inhomogeneities. Then the Rytov approximation for the log-amplitude variance (and also the variance of the phase fluctuations) has a wider range of applicability as compared with the isotropic case. Further, we formulate conditions that define the range of applicability of the presented formulas. We discussed the use of the log-amplitude variance as an estimate of scattering attenuation in anisotropic random media. Caution is required in the case $\gamma \ll 1$, because the attenuation of seismic primaries due to random diffraction and refraction in the presented approximation may then be small compared with the attenuation which is caused due to backscattering. It remains to be tested if a combination of 1-D Q -estimates which account for backscattering (such as obtained from the ODA approach) and the presented results for Q in 3-D anisotropic random media is more adequate to model Q -measurements in layered structures with finite lateral extent.

ACKNOWLEDGMENTS

This work was kindly supported by the sponsors of the *Wave Inversion Technology (WIT) Consortium* and by the Deutsche Forschungsgemeinschaft (contract SH55/2-2).

REFERENCES

- Beran, M. J. and McCoy, J. J. (1974). Propagation through an anisotropic random medium. *J. Math. Phys.*, 15:1901–1912.
- Dashen, R. (1979). Path integrals for waves in random media. *J. Math. Phys.*, 20:894–920.
- Harjes, H. P., Bram, K., Dürbaum, H. J., Gebrande, H., Hirschmann, G., Janik, M., Klöckner, M., Lüschen, E., Rabbel, W., Simon, S., Thomas, R., Tormann, J., and Wenzel, F. (1997). Origin and nature of crustal reflections: results from integrated seismic measurements at the KTB superdeep drill hole. *J. Geophys. Res.*, 102:18267–18288.
- Ikelle, L. T., Yung, S. K., and Daube, F. (1993). 2-d random media with ellipsoidal autocorrelation functions. *Geophysics*, 58:1359–1371.
- Ishimaru, A. (1978). *Wave Propagation and Scattering in random media*. Academic Press Inc., New York.
- Knollman, G. C. (1964). Wave propagation in a medium with random, spheroidal inhomogeneities. *J. Acoust. Soc. Am.*, 36:681–688.
- Komissarov, V. M. (1964). Amplitude and phase fluctuations and their correlation in the propagation of waves in a medium with random, statistically anisotropic inhomogeneities. *Soviet Physics-Acoustics*, 10:143–152.

- Kon, A. I. (1994). Qualitative theory of amplitude and phase fluctuations in a medium with anisotropic turbulent irregularities. *Waves Random Media*, 4:297–306.
- Lüschen, E., Sobolev, S., Werner, U., Söllner, W., Fuchs, K., Gurevich, B., and Hubral, P. (1993). Fluid reservoir (?) beneath the KTB drillbit indicated by seismic shear wave observations. *Geophys. Res. Lett.*, 20:923–926.
- Müller, T. M. and Shapiro, S. A. (2001). Seismic scattering attenuation estimates for the German KTB area derived from well-log statistics. *Geophys. Res. Lett.*, 28:3761–3764.
- Müller, T. M., Shapiro, S. A., and Sick, C. M. A. (2002). Most probable ballistic waves in random media: a weak fluctuation approximation and numerical results. *Waves Random Media*, 12:223–245.
- Ryberg, T., Fuchs, K., Egorkin, A. V., and Solodilov, L. (1995). Observation of high-frequency teleseismic p-n on the long-range quartz profile across northern Eurasia. *J. Geophys. Res.*, 100:18151–18163.
- Rytov, S. M., Kravtsov, Y. A., and Tatarskii, V. J. (1989). *Principles of statistical radiophysics, Volume IV: Wave Propagation Through Random Media*. Springer Verlag, Berlin, Heidelberg.
- Samuelides, Y. (1998). Velocity shift using the Rytov approximation. *J. Acoust. Soc. Am.*, 105:2596–2603.
- Sato, H. and Fehler, M. (1998). *Seismic wave propagation and scattering in the heterogeneous earth*. AIP press, New York.
- Shapiro, S. A. and Hubral, P. (1999). *Elastic waves in random media*. Springer, Berlin.
- Shapiro, S. A. and Kneib, G. (1993). Seismic attenuation by scattering: theory and numerical results. *Geophys. J. Int.*, 114:373–391.
- Tittgemeyer, M., Wenzel, F., Ryberg, T., and Fuchs, K. (1999). Scales of heterogeneities in the continental crust and upper mantle. *PAGEOPH*, 156:29–52.
- Tripathi, J. N. (2001). Small-scale structure of lithosphere-asthenosphere beneath Gauribidanur seismic array deduced from amplitude and phase fluctuations. *J. Geodynamics*, 31:411–428.
- Wagner, G. S. (1998). Local wave propagation near the San Jacinto fault zone, southern California: Observations from a three-component seismic array. *J. Geophys. Res.*, 103:7231–7246.
- Wu, R. S. and Flatté, S. M. (1990). Transmission fluctuations across an array and heterogeneities in the crust and upper mantle. *PAGEOPH*, 132:175–192.
- Wu, R. S., Xu, Z., and Li, X. P. (1994). Heterogeneity spectrum and scale-anisotropy in the upper crust revealed by the German continental deep-drilling (KTB) holes. *Geophys. Res. Lett.*, 21:911–914.